

KLOE results in kaon physics and prospects for KLOE–2

E. Czerwiński on behalf of KLOE and KLOE–2 collaborations*

Institute of Physics, Jagiellonian University, Cracow, Poland

Abstract

The ϕ -factory DAΦNE offers a possibility to select pure kaon beams, charged and neutral ones. In particular, neutral kaons from $\phi \rightarrow K_S K_L$ are produced in pairs and the detection of a K_S (K_L) tags the presence of a K_L (K_S). This allows to perform precise measurements of kaon properties by means of KLOE detector. Another advantage of a ϕ -factory consists in fact that the neutral kaon pairs are produced in a pure quantum state ($J^{PC} = 1^{--}$), which allows to investigate CP and CPT symmetries via quantum interference effects, as well as the basic principles of quantum mechanics.

A review of the most recent results of the KLOE experiment at DAΦNE using pure kaon beams or via quantum interferometry is presented together with prospects for kaon physics at KLOE–2.

Keywords: discrete symmetries, quantum mechanics, interferometry, kaon, DAΦNE, KLOE, KLOE–2

1. KLOE experiment at DAΦNE collider

The e^+e^- collider and ϕ -factory DAΦNE is placed in National Laboratory in Frascati (LNF-INFN, Italy). Electrons and positrons are accelerated in linac, then

stored and cooled in an accumulator and finally transferred in bunches into separated storage rings with two interaction points [1]. A schematic view of DAΦNE complex is presented in Fig. 1. The collider was de-

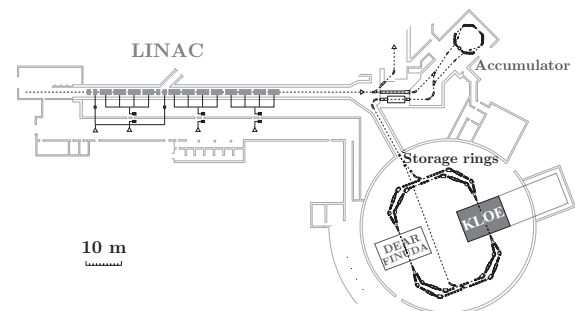


Figure 1: Scheme of the DAΦNE complex. A position of KLOE detector at one of two interaction points is also presented. Figure taken from [2].

*The KLOE collaboration: F. Ambrosino, A. Antonelli, M. Antonelli, F. Archilli, I. Balwierz, G. Bencivenni, C. Bini, C. Bloise, S. Bocchetta, F. Bossi, P. Branchini, G. Capon, T. Capussela, F. Ceradini, P. Ciambrone, E. Czerwiński, E. De Lucia, A. De Santis, P. De Simone, G. De Zorzi, A. Denig, A. Di Domenico, C. Di Donato, B. Di Micco, M. Dreucci, G. Felici, S. Fiore, P. Franzini, C. Gatti, P. Gauzzi, S. Giovannella, E. Graziani, M. Jacewicz, J. Lee-Franzini, M. Martemianov, M. Martini, P. Massarotti, S. Meola, S. Miscetti, G. Morello, M. Moulson, S. Müller, M. Napolitano, F. Nguyen, M. Palutan, A. Passeri, V. Patera, I. Prado Longhi, P. Santangelo, B. Sciascia, M. Silarski, T. Spadaro, C. Taccini, L. Tortora, G. Venanzoni, R. Versaci, G. Xu, J. Zdebek, and, as members of the KLOE–2 collaboration: D. Babusci, D. Badoni, V. Bocci, A. Budano, S. A. Bulychjev, L. Caldeira Balkeståhl, P. Campana, E. Dané, G. De Robertis, D. Domenici, O. Erriquez, G. Fanizzi, G. Giardina, F. Gonnella, F. Happacher, B. Höistad, L. Iafolla, E. Iarocci, T. Johansson, A. Kowalewska, V. Kulikov, A. Kupsc, F. Loddo, G. Mandaglio, M. Mascolo, M. Matsyuk, R. Messi, D. Moricciani, P. Moskal, A. Ranieri, C. F. Redmer, I. Sarra, M. Schioppa, A. Sciubba, W. Wiślicki, M. Wolke

signed to operate at the peak of ϕ resonance ($\sqrt{s} = m_\phi \approx 1019 \text{ MeV}$) producing ϕ mesons almost at rest ($\beta_\phi \approx 0.015$) since electrons and positrons collide with small transverse momenta. A ϕ meson decays mostly into kaon pairs (49% into K^+K^- and 34% into $K_S K_L$),

which makes a ϕ -factory the natural place for kaon physics studies.

During period from 2001 to 2006 KLOE has collected 2.5 fb^{-1} of integrated luminosity, which corresponds to about 6.6×10^9 kaon pairs [3]. The detector itself consists of two main components: a $\sim 3.3 \text{ m}$ long cylindrical drift chamber [4] with radius $\sim 4 \text{ m}$ surrounded by an electromagnetic calorimeter [5]. Both sub-detectors are inserted in a superconducting coil which produces an axial magnetic field of 0.52 T parallel to the beam axis. Fig. 2 shows a schematic view of KLOE detector. The KLOE drift chamber was designed

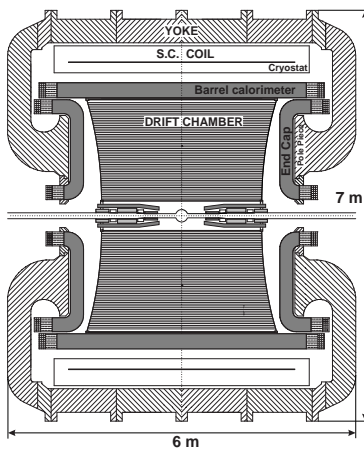


Figure 2: KLOE detector surrounded by superconducting coil. Collision point of electrons and positrons is in the spherical beam-pipe in the center of the detector. Figure adapted from [2].

to detect a sizable fraction of K_L decays (mean decay path of K_L meson is $\sim 3.4 \text{ m}$). The chamber is filled with a mixture of helium and isobutan (90% and 10%, respectively) and has about 52000 wires arranged in cylindrical layers with alternate stereo angles. Based on the reconstruction of charged track curvature it allows for a fractional momentum accuracy of $\sigma_p/p \approx 0.5\%$. The resolution of vertex reconstruction is about 1 mm , while overall spatial accuracy is below 2 mm . An electromagnetic calorimeter consists of a barrel and side detectors (*endcaps*) providing almost 4π coverage of solid angle. Each module of calorimeter is read out on both sides by set of photomultipliers. It is build of stack of 1 mm scintillating fiber layers glued between grooved lead foils. The obtained accuracy of energy and time measurement are $\sigma_E = 5.7\% / \sqrt{E[\text{GeV}]}$ and $\sigma(t) = 54 \text{ ps} / \sqrt{E[\text{GeV}]} \oplus 100 \text{ ps}$, respectively. Determination of the hit position in the plane transverse to the fiber direction is based on the analysis of signal amplitude distribution and the resolution is about 1 cm ,

while accuracy of longitudinal coordinate due to excellent time resolution amounts to $\sigma_z = 1.2 \text{ cm} / \sqrt{E[\text{GeV}]}$.

Since at KLOE kaons are produced in pairs from ϕ decay, reconstruction of K_S decay close to interaction region (clean selection of $K_S \rightarrow \pi^+\pi^-$, $\text{BR}=69\%$) allows for tagging of K_L presence. Having that and taking into account size of the detector itself makes KLOE an excellent place for K_L decay measurements. However, what is even more important, detection of K_L hit in calorimeter module tags the presence of K_S . This method makes KLOE an unique place to study pure K_S beams. It is used for measurement of $\text{BR}(K_S \rightarrow \pi^0\pi^0\pi^0)$ described in Section 2. It is also possible to study decays of both kaons in single event. Since both of them are produced in a pure quantum state ($J^{PC} = 1^{--}$), it is possible to study quantum interference effects for reaction $K_S K_L \rightarrow \pi^+\pi^-\pi^+\pi^-$, as it is shown in Section 3.

Recently KLOE-2, a successor of KLOE, has started data taking campaign in order to extend KLOE physics program [6]. Description of applied and planned upgrades together with physics prospect is presented in Section 4.

2. Preliminary result of $\text{BR}(K_S \rightarrow \pi^0\pi^0\pi^0)$ measurement

The decay $K_S \rightarrow \pi^0\pi^0\pi^0$ has not been observed so far. Up to now the best limit of branching ratio is $1.2 \cdot 10^{-7}$ [7], which is still about two orders of magnitude larger than theoretical predictions based on Standard Model ($\text{BR}_{SM} \sim 1.9 \cdot 10^{-9}$). Assuming the *CPT* invariance the described process allows for investigation of direct *CP* violation. At KLOE presence of K_S is tagged by K_L interaction with electromagnetic calorimeter (*K_L-crash*). Additional condition to select $K_S \rightarrow \pi^0\pi^0\pi^0$ decay candidates are presence of six neutral clusters (caused by gamma pairs from π^0 decays) and no charged tracks originating from interaction point. There are two main components for background reaction. Events of $K_S \rightarrow \pi^0\pi^0$ where two additional clusters are from splitting or accidental processes and $K_L \rightarrow \pi^0\pi^0\pi^0$, $K_S \rightarrow \pi^+\pi^-$ events. In the second case the K_L decay close to the interaction point mimics the K_S decay, while charged products of K_S due to interaction with quadrupoles simulate *K_L-crash* signal. As a first step for background reduction a kinematic fit was performed with 11 constrains of energy and momentum conservation, the kaon mass and velocity of six photons. Cut on obtained χ^2 values effectively reduce the background from false *K_L-crash* events without loose of signal events. For the rejection of events with splitted and/or accidental clusters a correlation between $\chi^2_{3\pi}$

and $\chi_{2\pi}^2$ variables was used. Both variables are evaluated with the most favorable cluster pairing in each case [7]. The quadratic sum of residuals between the π^0 mass and the invariant masses of three photon pairs formed from the six clusters is $\chi_{3\pi}^2$, while $\chi_{2\pi}^2$ is based on the invariant masses of two photon pairs and energy and momentum conservation for $\phi \rightarrow K_S K_L$ reaction, where $K_S \rightarrow \pi^0 \pi^0$. In addition, to improve the quality of the photon selection, a cut on $\Delta E = (m_\phi/2 - \sum E_{\gamma_i})/\sigma_E$ was applied, where γ_i stands for the i -th photon from four chosen in the $\chi_{2\pi}^2$ estimator and σ_E is the appropriate resolution. For two background clusters case ΔE is expected to be 0, while $\Delta E \approx m_{\pi^0}/\sigma_E$ for $K_S \rightarrow 3\pi^0$. Final cut was also applied on the minimal distance between photon clusters to refine rejection of events with splitted clusters. Result of this cut is shown in Fig. 3.

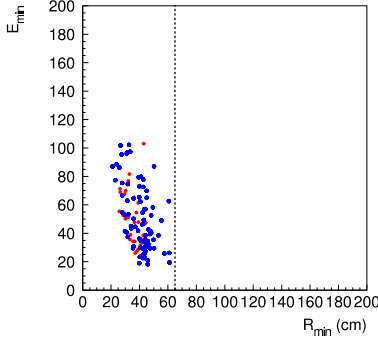


Figure 3: The distribution of minimal energy of the cluster versus minimal distance (R_{min}) between clusters in the event. The dashed line corresponds to the used R_{min} cut.

After preliminary cuts zero candidate events were obtained and zero events from Monte Carlo were observed. Data sample is based on 1.7 fb^{-1} integrated luminosity, while effective statistics of Monte Carlo is two times higher than data sample. This results in a new preliminary upper limit on branching ratio $BR(K_S \rightarrow 3\pi^0) < 2.9 \cdot 10^{-8}$ (corresponding to $|\eta_{3\pi^0}| = \left| \frac{A(K_S \rightarrow 3\pi^0)}{A(K_L \rightarrow 3\pi^0)} \right| < 0.009$), which is almost an order of magnitude better than the best limit obtained so far.

3. Interference with $K_S K_L \rightarrow \pi^+ \pi^- \pi^+ \pi^-$

At KLOE neutral kaons are produced in an entangled states from decay of ϕ meson with $J^{PC} = 1^{--}$

$$|i\rangle = \frac{1}{\sqrt{2}} \left\{ |K^0\rangle |\bar{K}^0\rangle - |\bar{K}^0\rangle |K^0\rangle \right\} = \frac{N}{\sqrt{2}} \left\{ |K_S\rangle |K_L\rangle - |K_L\rangle |K_S\rangle \right\}, \quad (1)$$

where $N = (1 + |\epsilon|^2)/(1 - \epsilon^2) \simeq 1$ is a normalization factor, with ϵ as the CP violating parameter in the mixing [8]. If one considers the case in which both kaons decay into identical final states, for example $K_S \rightarrow \pi^+ \pi^-$ and $K_L \rightarrow \pi^+ \pi^-$, the decay rate of the system is proportional to:

$$I(\pi^+ \pi^-, \pi^+ \pi^-, \Delta t) \propto e^{-\Gamma_L \Delta t} + e^{-\Gamma_S \Delta t} - 2e^{-\frac{\Gamma_L + \Gamma_S}{2} \Delta t} \cos(\Delta m \Delta t), \quad (2)$$

where Δm is the mass difference between K_L and K_S and Δt is the time difference between the decay of both kaons. This allows to study phenomena with increased accuracy due to interference pattern $2e^{-\frac{\Gamma_L + \Gamma_S}{2} \Delta t} \cos(\Delta m \Delta t)$. Eq. 2 implies that both kaons cannot decay at the same time, and it is an example of correlation of the type pointed out for the first time by Einstein, Podolsky and Rosen [9]. The initial state after ϕ meson decay spontaneously factorizes to an equal weight mixture of states $|K_S\rangle |K_L\rangle$ or $|K_L\rangle |K_S\rangle$ causing decoherence. The decoherence parameter ζ , which measures the amount of deviation from prediction of quantum mechanics, can be introduced in the following way:

$$I(\pi^+ \pi^-, \pi^+ \pi^-, \Delta t) \propto e^{-\Gamma_L \Delta t} + e^{-\Gamma_S \Delta t} - 2(1 - \zeta_{SL})e^{-\frac{\Gamma_L + \Gamma_S}{2} \Delta t} \cos(\Delta m \Delta t), \quad (3)$$

where value $\zeta = 0$ corresponds to the usual quantum mechanics case, while $\zeta = 1$ to the total decoherence (and different ζ values to intermediate situations between these two), as it is shown at the left plot in Fig. 4. In general ζ depends on the basis in which the initial

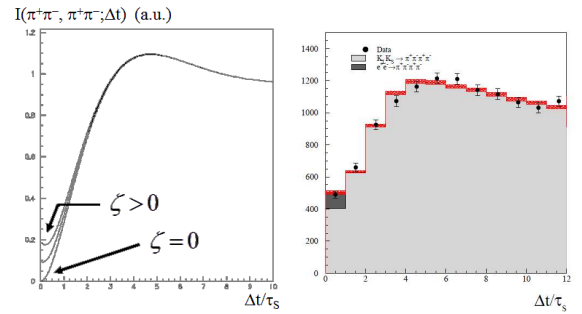


Figure 4: **Left:** The $I(\pi^+ \pi^-, \pi^+ \pi^-, \Delta t)$ distribution for quantum mechanic case ($\zeta = 0$), and for two greater than zero values of decoherence parameter. The biggest discrepancy is for Δt close to 0. The figure is taken from [8]. **Right:** Points denote experimental results, while fitted histogram shows results of the Monte Carlo simulation. The bin size corresponds to the time resolution $\sigma(\Delta t) \approx \tau_S$ [10].

state is expressed. At KLOE test of decoherence parameter was based on data analysis of $\approx 1.5 \text{ fb}^{-1}$ [10].

Selection of the signal events $\phi \rightarrow K_S K_L \rightarrow \pi^+ \pi^- \pi^+ \pi^-$ requires two vertexes, each with two opposite-curvature tracks inside the drift chamber, with an invariant mass and total momentum compatible with the two neutral kaon decays. The experimental points were fitted with Eq. 3 modified with parameters expressing decoherence in different models described in [8, 10]. The fit was performed taking into account resolution and detection efficiency, the background from coherent and incoherent K_S regeneration on the beam pipe wall, and the small contamination from the non-resonant $e^+ e^- \rightarrow \pi^+ \pi^- \pi^+ \pi^-$ channel. The determined experimental distribution of the $\phi \rightarrow K_S K_L \rightarrow \pi^+ \pi^- \pi^+ \pi^-$ intensity as a function of the absolute value of Δt is shown on the right plot in Fig. 4. The results:

$$\begin{aligned} \zeta_{SL} &= (0.3 \pm 1.8_{stat} \pm 0.6_{syst}) \cdot 10^{-2}, \\ \zeta_{00} &= (1.4 \pm 9.5_{stat} \pm 3.8_{syst}) \cdot 10^{-7}, \end{aligned} \quad (4)$$

show no deviation from quantum mechanics [10].

4. KLOE-2

The physics program of KLOE was related to the good accuracy of reconstruction of K_L decays in large fiducial volume, while at KLOE-2 an increased interest will be focused on the physics close to the interaction point (IP) as rare K_S decays, $K_S - K_L$ interference, multi-lepton events, as well as η , η' and K^\pm decays. More details about whole KLOE-2 physics program can be found in Ref. [6].

The new interaction region of electron and positron beams based on the Crabbed Waist compensation of the beam-beam interaction together with large Piwinski angle and small beam sizes at the crossing point was successfully commissioned in 2011 [11]. This modification allows to increase delivered luminosity (with unchanged beam current) by a factor of three with respect to the performance reached before the upgrade. During next 3-4 years of data taking with the KLOE-2 detector it is planned to collect $\sim 20 \text{ fb}^{-1}$ of integrated luminosity.

The detector itself was upgraded with two pairs of small angle tagging devices [12] to detect low (Low Energy Tagger - LET) [13] and high (High Energy Tagger - HET) energy $e^+ e^-$ originated from $e^+ e^- \rightarrow e^+ e^- X$ reactions. This tagger system will be used for $\gamma\gamma$ physics studies. First commissioning run of KLOE-2 has started in 2011. After collection of $\sim 5 \text{ fb}^{-1}$ the second phase of upgrade will start. In this step a light-material Inner Tracker detector based on the Cylindrical GEM technology will be installed in the region between the beam pipe and the drift chamber to improve

charged vertex reconstruction and to increase the acceptance for low transverse momentum tracks [14, 15]. Crystal calorimeters (CCALT) will cover the low polar θ angle region to increase acceptance for very forward electrons and photons down to 8° [16]. A new tile calorimeter (QCALT) will be used for the detection of photons coming from K_L decays in the drift chamber [17].

The tagging system is made of two different detectors which are already installed and ready for the data taking. Near the interaction region inside KLOE the small calorimeters (LET) consisting of LYSO crystals read out by silicon photomultipliers are placed. They will be used for measurements of electrons and positrons from $\gamma\gamma$ interaction within energy range from 160 to 230 MeV with an accuracy of $\sigma_E \sim 10\%$ [12]. At the distance of 11 m from the interaction point in the bending section of DAΦNE, the HET detectors are placed. They provide the measurement of the displacement of the scattered e^+ or e^- with respect to the main orbit. These position detectors consist of 30 small BC418 scintillators $3 \times 3 \times 5 \text{ mm}^3$ each and provides a spatial resolution of 2 mm (corresponding to momentum resolution of $\sim 1 \text{ MeV}$) for e^+/e^- with energy higher than 400 MeV.

The main part of KLOE-2 physics program [6] is concentrated in K_S , η and charged kaon decays as well as kaon interferometry. These events are produced close to the interaction point (IP), requiring an optimization of the detection for low momentum tracks coming from the IP. This is the purpose of installation of the Inner Tracker detector. It is based on a novel technology of fully cylindrical GEM (Gas Electron Multiplier) detectors [14, 15]. Each of its four concentric layers provides 2 coordinates, while the third is determined by the known radius of the layer. Each layer is a triple-GEM chamber with cathode and anode made of thin polyimide foils. The innermost layer will be placed 15 cm from the beam line, which corresponds to $20 \tau_S$ in order not to spoil the $K_L K_S$ interference, while the outermost layer is located close to the internal wall of the Drift Chamber.

The comparison between results obtained with present spatial resolution and after installation of Inner Tracker for decoherence studies (discussed in Section 3) is presented in Fig. 5. An improved sensitivity on decoherence parameters of about one order of magnitude is expected with an integrated luminosity of $\sim 20 \text{ fb}^{-1}$ and the use of Inner Tracker.

In order to improve measurements of the rare kaon, η , and η' decays two additional calorimeters QCALT and CCALT will be installed. QCALT composed by a sam-

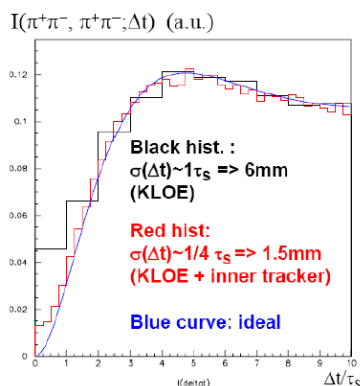


Figure 5: Comparison of the $I(\pi^+\pi^-, \pi^+\pi^-, \Delta t)$ distribution obtained with KLOE resolution and after Inner Tracker insertion based on the Monte Carlo simulation.

pling of 5 layers of 5 mm thick scintillator tiles alternated with 3.5 mm thick tungsten plates will constitute a 1 m long dodecagonal structure covering the region of the new quadrupoles inside the KLOE detector. The active part of each plane is divided into twenty tiles of about 5×5 cm² area with 1 mm diameter WLS fibers embedded in circular grooves. Silicon photomultipliers of 1 mm² area are used for readout each fiber [17]. In addition, crystal calorimeters (CCALT) shaped as two small barrels of LYSO crystals will cover the low polar angle region very close to the IP to increase acceptance for very forward photons. Readout system with silicon photomultipliers will be used aiming to achieve a timing resolution between 300 and 500 ps for 20 MeV photons [16].

5. Summary

KLOE experiment achieved already several significant and precise results in kaon physics [3], due to the unique possibility of producing pure K_L , K_S and K^\pm beams. Moreover, there are still ongoing investigation, like search of $K_S \rightarrow 3\pi^0$ decay presented here. The success of the DAΦNE upgrade motivated the start-up of a new experiment KLOE-2 which aims to complete and extend the KLOE physics program. LET and HET detectors have been already installed and the first phase of new data taking campaign has started. After collection of about 5 fb^{-1} of data new set of detectors will be installed (Inner Tracker, QCALT and CCALT calorimeters) for precise measurements of rare decays of kaon, η and η' , as well as CP and CPT tests and kaon interferometry studies. The expected total integrated luminosity collected by KLOE-2 should be about 20 fb^{-1} . The

accuracy in the measurements is expected in most cases to be improved by about one order of magnitude [6].

References

References

- [1] The ϕ -factory Study Group *Proposal for a ϕ -factory*, LNF-90/031 (R) (1991).
- [2] P. Franzini and M. Moulson, *Ann. Rev. Nucl. Part. Sci.* **56** (2006) 207.
- [3] F. Bossi, E. De Lucia, J. Lee-Franzini, S. Miscetti, M. Palutan and KLOE Collaboration, *Rivista del Nuovo Cimento* Vol.31, N.10 (2008).
- [4] M. Adinolfi, *et al.*, *Nucl. Instrum. Meth. A* **461** (2001) 25-28.
- [5] M. Adinolfi *et al.*, *Nucl. Instrum. Meth. A* **482** (2002) 364.
- [6] G. Amelino-Camelia *et al.*, *Eur. Phys. J. C* **68** (2010) 619-681.
- [7] F. Ambrosino *et al.*, *Phys. Lett. B* **619** (2005) 61-70.
- [8] *Handbook on neutral kaon interferometry at a Phi-factory*, editor: A. Di Domenico, Frascati Physics Series **43** (2007).
- [9] A. Einstein, B. Podolsky, N. Rosen, *Physical Review* **47** (1935) 777.
- [10] A. Di Domenico *et al.* [KLOE Collaboration], *J. Phys. Conf. Ser.* **171** (2009) 012008.
- [11] M. Zobov *et al.*, *Phys. Rev. Lett.* **104** (2010) 174801-174806.
- [12] F. Archilli *et al.*, *Nucl. Instr. & Meth. A* **617** (2010) 266.
- [13] D. Babusci *et al.*, *Nucl. Instr. & Meth. A* **617** (2010) 81.
- [14] KLOE-2 Collaboration, F. Archilli *et al.*, LNF-10/3(P) INFN-LNF, arXiv:1002.2572
- [15] A. Balla *et al.*, *Nucl. Instr. & Meth. A* **604** (2009) 23.
- [16] M. Cordelli *et al.*, *Nucl. Instr. & Meth. A* **617** (2010) 109.
- [17] M. Cordelli *et al.*, *Nucl. Instr. & Meth. A* **617** (2010) 105.